Published in final edited form as:
Nature. 2014 February 13; 506(7487): 249–253. doi:10.1038/nature12868.

RecA bundles mediate homology pairing between distant sisters during DNA break repair

Christian Lesterlin, **Graeme Ball**, **Lothar Schermelleh**, and **David J. Sherratt**
Department of Biochemistry, University of Oxford, Oxford, OX1 3QU, UK

Abstract

DNA double-strand break (DSB) repair by homologous recombination (HR) has evolved to maintain genetic integrity in all organisms[1]. Although many reactions that occur during HR are known[1-3], it is unclear where, when and how they occur in cells is lacking. Here, by using conventional and super-resolution microscopy we describe the progression of DSB repair in live *Escherichia coli*. Specifically, we investigate whether HR can occur efficiently between distant sister loci that have segregated to opposite halves of an *E. coli* cell. We show that a site-specific DSB in one sister can be repaired efficiently using distant sister homology. After RecBCD processing of the DSB, RecA is recruited to the cut locus, where it nucleates into a bundle that contains many more RecA molecules than can associate with the two ssDNA regions that form at the DSB. Mature bundles extend along the cell long axis in the space between the bulk nucleoid and the inner membrane. Bundle formation is followed by pairing in which the two ends of the cut locus relocate at the periphery of the nucleoid and together move rapidly towards the homology of the uncut sister. After sister locus pairing, RecA bundles disassemble and proteins that act late in HR are recruited to give viable recombinants 1-2 generation time equivalents after formation of the initial DSB. Mutated RecA proteins that do not form bundles are defective in sister pairing and in DSB-induced repair. The work reveals an unanticipated role of RecA bundles in channeling the movement of the DNA DSB ends, thereby facilitating the long-range homology search that occurs before the strand invasion and transfer reactions.

Keywords

Escherichia coli; homologous recombination; double-strand break repair; chromosome segregation; super resolution microscopy

Although repair of DSBs by HR is efficient in *E. coli*, it is not known whether HR events are restricted to the ~15 min period in which sister loci remain in close association after replication[4,5], or whether HR can occur between distant segregated sister loci (~1.3 μm apart). To test whether segregated distant sisters can undergo recombination when a site-specific DSB was introduced into one sister, ~1 Mbp from the replication *oriC*, we expressed small amounts of unstable I-SceI endonuclease[6], so that most cells had only one

Correspondence and requests for materials should be addressed to DJ.S. (david.sherratt@bioch.ox.ac.uk)..

AUTHOR CONTRIBUTIONS DJ.S and C.L conceived the project, interpreted the data and wrote the paper. C.L designed and undertook experiments. G.B. developed analytical tools for microscopy data and provided advice on the manuscript. L.S. provided expertise on 3D-SIM and advice on the manuscript.

SUPPLEMENTARY INFORMATION is available in the online version of the paper.

AUTHOR INFORMATION Author Information Reprints and permissions information is available at www.nature.com/reprints.

Europe PMC Funders Author Manuscripts

of two sisters cleaved, and repaired the DSB efficiently in reactions that required RecABCD (Fig. 1 and Extended Data Fig. 1).

Fluorescent ParB-protein binding to DNA on either side of the cut site allowed us to monitor the fate of cut and uncut loci. After DSB induction, loss and randomized positioning of foci occurred, when compared to the uncut control, in which 1-focus cells had the focus displaced slightly from midcell and 2-focus cells had the foci on either side of midcell. Time-lapse analysis showed focus pairing, accompanied by increased fluorescence, and focus-loss, dependent on RecBCD degradation; events absent in wild-type cells (Fig. 1a, c and Extended Data Fig. 1a, 2). RecABCD-dependent sister pairing occurred on average ~100 min after induction of I-SceI expression and persisted for ~50 min before sister re-segregation (Fig. 1a). The two ends of the DSB remained in proximity after cutting and during subsequent processing, supporting schemes in which both DNA ends are engaged in HR repair (Fig. 1c and Extended Data Fig. 2a), as reported for eukaryotic repair[7]. The behavior of fluorescent foci marking each of the cut ends was similar, with the foci moving to the cell periphery after cutting (compare Fig. 1a and Extended Data Fig. 1d; Fig. 1b). RecBCD processing of the DSB was bidirectional consistent with efficient loading of RecBCD complexes onto both ends of the break. The rate of DNA degradation in the absence of RecA was ~190 bp/s per RecBCD complex, eventually leading to complete nucleoid degradation (Fig. 1c, d and Extended Data Fig. 2b, c; Video S1; Supplementary discussion).

RecBCD-dependent recruitment of RecA to the DSB was assayed in cells expressing a C-terminal fusion of RecA to green fluorescent protein (GFP)[8] and wild-type RecA, both expressed from wild-type chromosomal *recA* promoters. These cells exhibited wild-type repair and recombination, whereas those expressing RecA-GFP alone were not fully repair-proficient (Extended Data Fig. 3a)[8]. Prior to DSB-induction, ~95% of cells showed RecA-GFP fluorescence uniformly distributed throughout the cell, with ~5% of cells having fluorescent spots that were not associated with a marked locus (21% colocalization) (Extended Data Fig. 3b). After DSB induction, fluorescent RecA spots appeared close to or coincident with one of the two marked sister loci (64% colocalization; Fig. 2a, b). The transient RecA spots nucleated rapidly into filamentous structures that we term RecA-bundles, which had formed their maximum length by ~13 min and most often extended along the cell (Fig. 2c, d; Video S2). The DSB-induced stimulation of RecA spot and bundle formation required RecBCD processing of the cut ends (Fig. 2e).

Rapid sister locus pairing occurred ~47 min after RecA bundle formation (Fig. 2f, g). During this period, no consistent changes in bundle architecture occurred and no significant turnover of RecA within the mature bundle structure was observed by FRAP (Fluorescence Recovery After Photobleaching; Extended Data Fig. 3c; Video S3). Once initiated, sister focus pairing was rapid (within 5 min in 69% of events) and was asymmetric with the cut sister traveling ~84% of the ~1.3 μm distance between sister loci (Fig. 2h). Although the cut and uncut loci showed similar diffusion coefficients (D_{app}), the movement of the cut locus was 5-7-fold more directional than the uncut locus, indicative of channeling of the movement of the cut locus (Fig. 2h; Extended Data Fig. 4a).

We propose that nucleation of RecA onto the ssDNA ends formed by RecBCD processing at the DSB triggers polymerization of RecA into bundles, which are required for pairing between distant sisters. RecA bundles disassembled rapidly and unidirectionally ~17 min after pairing of the sister loci, possibly triggered by the loss of the ssDNA-RecA ends upon strand invasion (Fig. 2i and j; Video S2). After pairing, sisters re-segregated and cells re-established normal growth, cell division and chromosome segregation (summary diagram Fig. 2k). In parallel, we have shown that DSB-induction and bundle formation are followed

by the recruitment of PriA and RecG recombination proteins that promote replication restart and recombination intermediate processing. In contrast, RecN was recruited early to the break (Extended Data Fig. 4b and c; Supplementary Discussion). Bundles of wild-type RecA that formed in response to DSBs were also observed in fixed cells using immunocytochemistry and in live cells with a more functional RecA803-RFP fusion (Extended Data Fig. 5)[9]. Furthermore, repair-deficient cells expressing RecAK72A-GFP, which fails to bind ATP, did not form spots or bundles, whereas cells expressing RecAK72R-GFP, which binds ATP but is hydrolysis impaired[10], formed weak spots close to the cut locus (0.49 ±0.2 μm), consistent with RecAK72R forming filaments on ssDNA and initiating strand transfer *in vitro*[10]. Nevertheless, the RecAK72R-GFP spots failed to nucleate bundles, and *recAK72R* cells did not show sister pairing and were repair-deficient (Extended Data Fig. 5). These data demonstrate that RecA bundles are physiologically relevant forms of RecA that are critical for HR repair between distant regions of homology.

To gain more insight into RecA bundle architecture and function, we used super-resolution three-dimensional structured illumination microscopy (3D-SIM) and live cell time-lapse imaging (Fig. 3). RecA-bundles most frequently adopted overall longitudinal trajectories, with some radial writhing (Video S4) and were located between the surface of the nucleoid and the inner membrane. Bundles may be excluded from the nucleoid because of their size, as are ~20 nm diameter ribosomes[11], and their localization at the cell membrane could arise because activated forms of RecA may associate with phospholipid membranes[12]. 3D-SIM showed that 91% of bundles were associated with at least one sister focus, confirming the earlier data (Fig. 3a; Extended Data Fig. 3b; Video S5). Bundles were on average ~1.4 μm long and typically consisted of a ~160 nm thick central region bounded by thinner (≤120 nm) extensions (Extended Data Fig. 3b). 3D SIM-time-lapse analysis revealed that the central region was relatively immobile whereas the thin extensions moved rapidly and appeared to probe the inner cell compartment (Fig. 3a; Video S6-7).

Bundles contained ~70% of the normal pool of cellular RecA, estimated to be ~4640 ±1908 molecules/cell, independently of the presence of spots or bundles (Fig. 3b, c and Extended Data Fig 3d; Supplementary Discussion). The rate of RecA incorporation into DSB-induced bundles was ~4 monomer/s, which compares with an *in vitro* rate of 0.5-7 monomer/s/DNA end, or nucleation point[13,14]. We estimate that >85 % of RecA molecules present in bundles are likely to be DNA-free and additional to the two presynaptic ssDNA-RecA filaments that we propose nucleate bundle formation (Supplementary Discussion). DNA-free RecA filaments and bundles can form *in vitro*[15,16], and have a similar architecture to that of RecA-DNA filaments[17-19] . The observed ~1.4 μm length of RecA bundles is less than the ~2.5 μm long twin filament that would form from ~3200 RecA molecules nucleating onto the two ssDNA ends at the break. Thus, RecA bundles may contain lateral filaments, potentially explaining the thicker central regions of the bundles. RecA bundles have been observed in previous light microscopy and EM studies, and have been shown to appear in response to DNA damage in *E. coli*[8,20,21], and in response to DSBs in *Bacillus subtilis*[22]. In the latter case spots appeared close to the site of the DSB and extended into longitudinal bundles, whose formation was dependent on the *B. subtilis* RecBCD orthologue, AddAB. Nevertheless, their physiological significance has been unclear, though it was proposed that RecA bundles are inactive storage forms[8,18].

Our data demonstrate conclusively that DSB-induced homology pairing can occur between distant segregated sister loci, and therefore HR is not restricted to the ~15 min cohesion period following replication. We propose that RecA bundles, actively facilitate the process of locus pairing between distant sisters, thereby leading to the eventual homology-directed strand invasion. The observation that sister pairing is not necessarily accompanied by bundle shortening suggests that the DNA ends move along the bundle. This could be driven by

sliding between RecA filaments within the bundle as proposed for ParM-mediated DNA movement[23], a treadmilling mechanism in which RecA filament growth at the leading edge and disassembly in the region of the cut locus could lead to rapid pairing, or a process in which a motor-like protein associated with the cut ends moves along the bundle, akin to other motor proteins moving along cytoskeletal elements. Mechanisms in which pairing arises in part as 'passive' 1D diffusion along a restraining bundle, would still require a process that directs the cut locus towards the opposite side of the cell. In any of these scenarios, the channeled movement of the cut ends would be 'blind' to the uncut sister until a local homology search accompanied by strand invasion generated the strand transfer complex whose processing leads to completed recombination products. It follows therefore that nucleation of a RecA spot into a bundle should occur irrespective of whether sister homology is present. Consistent with this, RecA bundles formed at similar frequencies regardless of whether sister homology was present (Extended Data Fig. 3e; Supplementary Discussion). The two–step mechanism we propose only needs to be used when sister homology is distant from the cut locus; immediately after replication, when sister loci remain in close proximity, DSB repair by HR might occur simply by the canonical mechanism of strand invasion and transfer.

The formation of RecA bundles and equivalent structures in other organisms may be a general mechanism for channeling the movement of damaged DNA loci, thereby enabling a genome-wide homology search in a cell compartment at the periphery of the nucleoid. Since other repair proteins are known to interact with RecA and its orthologues, bundles may promote the binding and movement of other players in DNA repair. In eukaryotes, HR may also fall into two classes defined by the distance the homology search needs to take. For example, allelic events between cohesed sisters and between paired homologues in meiosis do not involve distant pairing events. In contrast, non-allelic HR events, or those between homologous mitotic chromosomes may use processes that involve the equivalent of RecA bundles to facilitate the homology search, a process that may take longer, as observed for inter-homologue HR intermediates[7].

MATERIAL AND METHODS

Bacterial strains and growth

All strains are derivatives of *E. coli* K12 TB28 (MG1655, Δ*lacIZYA*[24]). Cells were grown at 30°C in M9 media supplemented with 0.2% glucose. Ampicillin (100 μg/ml), kanamycin (50 μg/ml), chloramphenicol (20 μg/ml) and tetracycline (10 μg/ml) were added when required. Expression of I-SceI endonuclease from an arabinose inducible promoter[25] was induced by the addition of 0.2% arabinose. Intracellular localisation of chromosomal loci flanking the *I-SceI*^{CS} cut site was visualized by fluorescent wide-field microscopy using two distinct ParB/*parS* systems[26]. Mutations were generally constructed by λ-Red recombination[27] and further introduced into the strain of interest by P1 transduction. When needed, the DNA region between the two *frt* sites (*cam/kan* resistance genes) was removed using Flp recombinase expressed from pCP20[27].

Microscopy sample preparation

All microscopy experiments were performed on live cells growing in exponential phase (A_{600}~0.1-0.2). Cells were transferred from liquid culture to a slide mounted with 1% agarose in M9 glucose 0.2% medium and incubated during microscopy at the required temperature using an incubation chamber. 3D-structured illumination microscopy (3D-SIM) snapshots were performed at 24 °C with cells covered with precision cover glass thickness No. 1.5H (170 μm ±5 μm; Marienfeld Superior) using immersion oil with a refractive index of 1.512 to minimise spherical aberration. For time-lapses after DSB induction, arabinose

0.2% was added to the liquid culture for 30 min before the cell were mounted on the slide. Nucleoids were visualized using 4 μg/ml 4′,6-diamidino-2-phenylindole (DAPI), and cells membrane were visualized using 1 μg/ml FM4-64 (Life Technologies).

Wide-field microscopy, 3D-structured illumination microscopy and FRAP imaging

Conventional wide-field fluorescence microscopy was carried out on an Eclipse TE2000-U microscope (Nikon), equipped with a 100x/1.4 oil PlanApo objective and either a Cool-Snap HQ CCD or a QuantEM camera (Photometrics), and using Metamorph software for image acquisition. Super-resolution 3D-SIM imaging as well as conventional wide-field imaging was performed on a DeltaVision OMX V3 (Applied Precision/GE Healthcare) equipped with a Blaze SIM module, a 60x/1.42 oil UPlanSApo objective (Olympus), 405 nm and 488 nm and 593 nm diode lasers and three sCMOS cameras (PCO). The fast-live mode enabled ultra-high speed illumination and simultaneous or sequential acquisition of multiple-color 3D stacks of RecA-GFP/DAPI, RecA-GFP/FM4-64, RecA-GFP/mCherry or RecA-GFP alone. For each color, the raw 3D-SIM stacks were composed of 225 images (512×512 pixels) consisting of 15 z-sections (125 nm z-distance, sample thickness of 1.750 μm), with 15 images per z-section with the striped illumination pattern [28,29] rotated to the three angles (−60°, 0°, +60°) and shifted in five phase steps. Acquisition settings were as follows: RecA-GFP, 2-5 ms exposure with 488 nm laser (attenuated to 10% transmission); DAPI, 20 ms exposure with 405 nm laser (100% transmission); FM4-64, 30 ms exposure with 593 nm laser (100% transmission). Total acquisition times per stack were 1.8 s for RecA-GFP, and ~10 s for RecA-GFP/DAPI and RecA-GFP/FM4-64. Note that simultaneous imaging of RecA-GFP and DSe (ParB-mCherry) was performed in 3D-SIM mode for RecA-GFP and conventional wide-field for ParB-mCherry. The 3D-SIM raw data was computationally reconstructed with SoftWoRx 6.0 (Applied Precision) using Wiener filter settings 0.002 and channel specifically measured optical transfer functions to generate a super-resolution 3D image stack with a lateral (x-y) resolution of 100-130 nm (wavelength-dependent) and an axial (z) resolution of ~300 nm. In the reconstruction process the pixel size is halved from 80 nm to 40 nm and the pixel number doubled in order to meet the Nyquist sampling criterion. The number of pixels in the DSe conventional images were doubled using Priism (Image Visualization Environment, http://msg.ucsf.edu/IVE/) in order to merge with 3D-SIM images. A constrained iterative 3D image deconvolution was applied to conventional wide-field data in SoftWorX 6.0. Images from the different color channels were registered with alignment parameter obtained from calibration measurements with 0.2 μm diameter TetraSpeck beads (Life Technologies) using the OMX Editor software (Chris Weisiger & John Sedat, UCSF; unpublished). FRAP experiments were performed with an UltraVIEW VoX spinning disk confocal system with Photokinesis module (PerkinElmer) assembled on an IX8 microscope (Olympus) equipped with an C9100-13 EMCCD camera (Hamamatsu) and a 100x/1.4 oil PlanApo objective (Olympus). Photobleaching of a small diffraction-limited spot was carried out with a focused 488 nm laser beam (100 ms with AOTF set to 50% transmission). Fluorescence intensity measurements of the unbleached and bleached regions were performed using ImageJ (rsbweb.nih.gov/ij/). Values were normalized to those of initial prebleaching images.

Snapshot and time-lapse analysis

Snapshot analysis was performed with the MicrobeTracker suite[30] extended by custom MATLAB routines which we specifically developed to generate focus positioning dotplots, histograms of 0/1/2-focus cell fractions, 2-color cell-type counting, inter-sister-focus distance (ISD), USe-DSe distance, focus position along the cell long X-axis (length) and short Y-axis (width). Distributions of DSe foci along the cell diameter presented Fig. 1b were performed by subdividing cells into five cell slices of equivalent areas as indicated in Meile *et al.*, (2011)[31]. Stoichiometry of RecA was determined by convolving the total

fluorescence in *recA-GFP* cells and compare it to that of *mukB-GFP* cells for which MukB stoichiometry is known[32]. Total intracellular fluorescence intensity distribution analysis was performed on images resulting from the average projection of 15 z-sections (125 nm z-distance) corresponding to a sample thickness of 1.750 μm, using MicrobeTracker. Our estimate of RecA stoichiometry is in the range of previous estimates[33-36]. Fluorescent particle tracking during long time-lapses (>30 s/frame) was performed using a semi-automated custom MATLAB routine as previously described[37]. Mean Square Displacement (MSD) in X and Y dimensions and directionality of movement were obtained by running the View5D plug-in (ImageJ) on short time-lapses (300 s; 5 s/frame). The apparent 2D diffusion coefficient (D_{app}) was calculated from the initial slope of MSD plotted against time using $MSD_{XY}=4(D_{app})t$. The directionality of movement reflects the fraction of the overall displacement ($\Delta d_{1\text{-}t}$), compared to the total distance travelled by the focus ($\Delta d_1+\Delta d_2\ldots+\Delta d_t$) i.e., Directionality=($\Delta d_{1\text{-}t}/(\Delta d_1+\Delta d_2\ldots+\Delta d_t)$).

Immunocytochemistry

Cells were fixed in phosphate buffered saline with paraformaldehyde 5% (pH 7.2) and glutaraldehyde 0.06% and immobilized on poly-L-lysine slides (Poly-prep from Sigma-Aldrich), followed by treatment with lysozyme 1μg/ml. Immunocytochemistry was performed using rabbit anti-RecA polyclonal antibodies (Abnova), which were revealed using anti-rabbit secondary antibodies conjugated to Alexa 594 (Life Technologies). Coverslips were mounted with Vectashield mounting medium (Vector Laboratories).

Flow cytometry

Cells were grown in M9 glucose at 30°C and sampled in late stationary phase, exponential phase (A_{600}~0.15) and 3 hours after incubation with cephalexin and rifampicin (run-out). Cell samples were prepared as described[38] except that Syto16 (Life Technologies) was used to stain DNA. Analysis was performed on FACScalibur flow cytometer (BD Biosciences). Data files were analyzed using CellQuest (BD Biosciences) and Weasel (WEHI; http://www.wehi.edu.au/).

Construction of I-SceI system for induction of site-specific DSB into the *E. coli* chromosome

The Rec^+ strain, in which DSB were initially induced corresponds to TB28 with both the *I-SceI* cut site and the gene encoding the *I-SceI* endonuclease inserted into *codA-cynR* and *araB* chromosome loci, respectively. The *I-SceI*^{CS} cassette carries *frt-cam-parSP1-frt-3*χ^+*-I-SceI*^{CS}*-parSPMT1-3*χ^- where *I-SceI*^{CS} stands for the cut site (5′-TAGGGATAACAGGGTAAT-3′), +/− stand for the orientation of 5′-GCTGGTGG-3′ χ-sites[39] and *frt* indicates the Flp site-specific recombination sites. *parS* sites were amplified from pGBKD3-*parSPMT1* and pGBKD3-*parSP1* plasmids[40]. The cassette was integrated into *codA-cynR* intergenic region of MG1655 chromosome (356.6 kb) or into *ydeO-ydeP* intergenic region (1,581.7 kb) by λ-Red recombination[27] and further transferred by P1 transduction into TB28. The wild-type allele of a *I-SceI* gene under the control of arabinose inducible promoter (carried by pDL2655 plasmid described in White *et al.*, (2008)[39]) was fused to 1X*c-Myc* tag followed by the DAS+4-degron tag in its C-terminus[41] amplified from pROD60. This plasmid carrying a 6-aa linker, Myc tag, 2-aa linker and the DAS+4 degron tag (S A G S A A E Q K L I S E E D L S S A A N D E N Y S E N Y A D A S) was as described[42]. The *I-SceI-degron* construct was tested for its reduced efficiency to linearize a *I-SceI*$_{CS}$-carrying plasmid after induction with 0.2% arabinose *in vivo*. P_{ara} *I-SceI-frt-kan* or P_{ara}*I-SceI-degron-frt-kan* constructs were inserted in the *araB* gene (70 kb) of MG1655/pKD46 by the process of λ-Red recombination and further transferred into TB28 by P1 transduction. The *recA* gene with its P_{recA} promoter region were amplified from K12

genomic DNA and subsequently integrated downstream of *fhuB* gene on MG1655 chromosome (171 kb on the chromosome) by λ-Red recombination and transferred into TB28 by P1 transduction (referred as *fhuB::recA-cat*).

Supplementary Material

Refer to Web version on PubMed Central for supplementary material.

Acknowledgments

The work was supported by an EMBO Long-term fellowship to CL (LTF-535-2009); to a Wellcome Trust Programme Grant to DJS (WT083469MA) and by a Wellcome Trust Strategic Award (091911) supporting advanced microscopy at Micron Oxford (http://micronoxford.com). We thank Ian Dobbie for his generous support and advice on imaging. We thank David Leach and Stephen Kowalczykowski for the gift of strains and plasmids, Nelly Dubarry for critical reading of the manuscript and Mathieu Stouf for the gift of pMS11. We thank E. Birt and K. Prosser for preliminary experiments.

REFERENCES

1. Cromie GA, Connelly JC, Leach DR. Recombination at double-strand breaks and DNA ends: conserved mechanisms from phage to humans. Mol Cell. 2001; 8:1163–1174. [PubMed: 11779493]
2. Cox MM. Regulation of bacterial RecA protein function. Critical reviews in biochemistry and molecular biology. 2007; 42:41–63. doi:10.1080/10409230701260258. [PubMed: 17364684]
3. Dillingham MS, Kowalczykowski SC. RecBCD enzyme and the repair of double-stranded DNA breaks. Microbiol Mol Biol Rev. 2008; 72:642–671. Table of Contents, doi:10.1128/MMBR.00020-08. [PubMed: 19052323]
4. Lesterlin C, Gigant E, Boccard F, Espeli O. Sister chromatid interactions in bacteria revealed by a site-specific recombination assay. Embo J. 2012; 31:3468–3479. doi:emboj2012194 [pii]10.1038/emboj.2012.194. [PubMed: 22820946]
5. Reyes-Lamothe R, Possoz C, Danilova O, Sherratt DJ. Independent positioning and action of Escherichia coli replisomes in live cells. Cell. 2008; 133:90–102. doi:10.1016/j.cell.2008.01.044. [PubMed: 18394992]
6. Monteilhet C, Perrin A, Thierry A, Colleaux L, Dujon B. Purification and characterization of the in vitro activity of I-Sce I, a novel and highly specific endonuclease encoded by a group I intron. Nucleic Acids Res. 1990; 18:1407–1413. [PubMed: 2183191]
7. Bzymek M, Thayer NH, Oh SD, Kleckner N, Hunter N. Double Holliday junctions are intermediates of DNA break repair. Nature. 2010; 464:937–941. doi:10.1038/nature08868. [PubMed: 20348905]
8. Renzette N, et al. Localization of RecA in Escherichia coli K-12 using RecA-GFP. Mol Microbiol. 2005; 57:1074–1085. doi:10.1111/j.1365-2958.2005.04755.x. [PubMed: 16091045]
9. Handa N, Amitani I, Gumlaw N, Sandler SJ, Kowalczykowski SC. Single molecule analysis of a red fluorescent RecA protein reveals a defect in nucleoprotein filament nucleation that relates to its reduced biological functions. J Biol Chem. 2009; 284:18664–18673. doi:10.1074/jbc.M109.004895. [PubMed: 19419960]
10. Rehrauer WM, Kowalczykowski SC. Alteration of the nucleoside triphosphate (NTP) catalytic domain within Escherichia coli recA protein attenuates NTP hydrolysis but not joint molecule formation. J Biol Chem. 1993; 268:1292–1297. [PubMed: 8419331]
11. Bakshi S, Siryaporn A, Goulian M, Weisshaar JC. Superresolution imaging of ribosomes and RNA polymerase in live Escherichia coli cells. Mol Microbiol. 2012; 85:21–38. doi:10.1111/j.1365-2958.2012.08081.x. [PubMed: 22624875]
12. Garvey N, St John AC, Witkin EM. Evidence for RecA protein association with the cell membrane and for changes in the levels of major outer membrane proteins in SOS-induced Escherichia coli cells. J Bacteriol. 1985; 163:870–876. [PubMed: 3897198]

13. Bell JC, Plank JL, Dombrowski CC, Kowalczykowski SC. Direct imaging of RecA nucleation and growth on single molecules of SSB-coated ssDNA. Nature. 2012; 491:274–278. doi:10.1038/nature11598. [PubMed: 23103864]
14. Feinstein E, et al. Single-molecule studies of the stringency factors and rates governing the polymerization of RecA on double-stranded DNA. Nucleic Acids Res. 2011; 39:3781–3791. doi:10.1093/nar/gkr013. [PubMed: 21245047]
15. Brenner SL, Zlotnick A, Griffith JD. RecA protein self-assembly. Multiple discrete aggregation states. J Mol Biol. 1988; 204:959–972. [PubMed: 3065521]
16. DiCapua E, Schnarr M, Ruigrok RW, Lindner P, Timmins PA. Complexes of RecA protein in solution. A study by small angle neutron scattering. J Mol Biol. 1990; 214:557–570. doi:10.1016/0022-2836(90)90198-U. [PubMed: 2380987]
17. Chen Z, Yang H, Pavletich NP. Mechanism of homologous recombination from the RecA-ssDNA/dsDNA structures. Nature. 2008; 453:489–484. doi:10.1038/nature06971. [PubMed: 18497818]
18. Story RM, Weber IT, Steitz TA. The structure of the E. coli recA protein monomer and polymer. Nature. 1992; 355:318–325. doi:10.1038/355318a0. [PubMed: 1731246]
19. Yu X, VanLoock MS, Yang S, Reese JT, Egelman EH. What is the structure of the RecA-DNA filament? Current protein & peptide science. 2004; 5:73–79. [PubMed: 15078218]
20. Levin-Zaidman S, et al. Ordered intracellular RecA-DNA assemblies: a potential site of in vivo RecA-mediated activities. Proc Natl Acad Sci U S A. 2000; 97:6791–6796. doi:10.1073/pnas.090532397. [PubMed: 10829063]
21. Renzette N, Sandler SJ. Requirements for ATP binding and hydrolysis in RecA function in Escherichia coli. Mol Microbiol. 2008; 67:1347–1359. doi:10.1111/j.1365-2958.2008.06130.x. [PubMed: 18298444]
22. Kidane D, Graumann PL. Dynamic formation of RecA filaments at DNA double strand break repair centers in live cells. The Journal of cell biology. 2005; 170:357–366. doi:10.1083/jcb.200412090. [PubMed: 16061691]
23. Gayathri P, et al. A bipolar spindle of antiparallel ParM filaments drives bacterial plasmid segregation. Science. 2012; 338:1334–1337. doi:10.1126/science.1229091. [PubMed: 23112295]
24. Bernhardt TG, de Boer PA. Screening for synthetic lethal mutants in Escherichia coli and identification of EnvC (YibP) as a periplasmic septal ring factor with murein hydrolase activity. Mol Microbiol. 2004; 52:1255–1269. doi:10.1111/j.1365-2958.2004.04063.x. [PubMed: 15165230]
25. Guzman LM, Belin D, Carson MJ, Beckwith J. Tight regulation, modulation, and high-level expression by vectors containing the arabinose PBAD promoter. J Bacteriol. 1995; 177:4121–4130. [PubMed: 7608087]
26. Nielsen HJ, Ottesen JR, Youngren B, Austin SJ, Hansen FG. The Escherichia coli chromosome is organized with the left and right chromosome arms in separate cell halves. Mol Microbiol. 2006; 62:331–338. doi:10.1111/j.1365-2958.2006.05346.x. [PubMed: 17020576]
27. Datsenko KA, Wanner BL. One-step inactivation of chromosomal genes in Escherichia coli K-12 using PCR products. Proc Natl Acad Sci U S A. 2000; 97:6640–6645. [PubMed: 10829079]
28. Gustafsson MG, et al. Three-dimensional resolution doubling in wide-field fluorescence microscopy by structured illumination. Biophys J. 2008; 94:4957–4970. doi:10.1529/biophysj.107.120345. [PubMed: 18326650]
29. Schermelleh L, et al. Subdiffraction multicolor imaging of the nuclear periphery with 3D structured illumination microscopy. Science. 2008; 320:1332–1336. doi:10.1126/science.1156947. [PubMed: 18535242]
30. Sliusarenko O, Heinritz J, Emonet T, Jacobs-Wagner C. High-throughput, subpixel precision analysis of bacterial morphogenesis and intracellular spatio-temporal dynamics. Mol Microbiol. 2011; 80:612–627. doi:10.1111/j.1365-2958.2011.07579.x. [PubMed: 21414037]
31. Meile JC, et al. The terminal region of the E. coli chromosome localises at the periphery of the nucleoid. BMC microbiology. 2011; 11:28. doi:10.1186/1471-2180-11-28. [PubMed: 21288323]
32. Badrinarayanan A, Reyes-Lamothe R, Uphoff S, Leake MC, Sherratt DJ. In vivo architecture and action of bacterial structural maintenance of chromosome proteins. Science. 2012; 338:528–531. doi:10.1126/science.1227126. [PubMed: 23112333]

33. Stohl EA, et al. Escherichia coli RecX inhibits RecA recombinase and coprotease activities in vitro and in vivo. J Biol Chem. 2003; 278:2278–2285. doi:10.1074/jbc.M210496200. [PubMed: 12427742]
34. Sommer S, Boudsocq F, Devoret R, Bailone A. Specific RecA amino acid changes affect RecA-UmuD'C interaction. Mol Microbiol. 1998; 28:281–291. [PubMed: 9622353]
35. Sassanfar M, Roberts J. Constitutive and UV-mediated activation of RecA protein: combined effects of recA441 and recF143 mutations and of addition of nucleosides and adenine. J Bacteriol. 1991; 173:5869–5875. [PubMed: 1715863]
36. Karu AE, Belk ED. Induction of E. coli recA protein via recBC and alternate pathways: quantitation by enzyme-linked immunosorbent assay (ELISA). Mol Gen Genet. 1982; 185:275–282. [PubMed: 6283318]
37. Wang X, Lesterlin C, Reyes-Lamothe R, Ball G, Sherratt DJ. Replication and segregation of an Escherichia coli chromosome with two replication origins. Proc Natl Acad Sci U S A. 2011; 108:E243–250. doi:10.1073/pnas.1100874108. [PubMed: 21670292]
38. Lesterlin C, Pages C, Dubarry N, Dasgupta S, Cornet F. Asymmetry of chromosome Replichores renders the DNA translocase activity of FtsK essential for cell division and cell shape maintenance in Escherichia coli. PLoS Genet. 2008; 4:e1000288. doi:10.1371/journal.pgen.1000288. [PubMed: 19057667]
39. White MA, Eykelenboom JK, Lopez-Vernaza MA, Wilson E, Leach DR. Non-random segregation of sister chromosomes in Escherichia coli. Nature. 2008; 455:1248–1250. doi:10.1038/nature07282. [PubMed: 18972020]
40. Espeli O, Mercier R, Boccard F. DNA dynamics vary according to macrodomain topography in the E. coli chromosome. Mol Microbiol. 2008; 68:1418–1427. doi:10.1111/j.1365-2958.2008.06239.x. [PubMed: 18410497]
41. McGinness KE, Baker TA, Sauer RT. Engineering controllable protein degradation. Mol Cell. 2006; 22:701–707. doi:10.1016/j.molcel.2006.04.027. [PubMed: 16762842]
42. Reyes-Lamothe R, Sherratt DJ, Leake MC. Stoichiometry and architecture of active DNA replication machinery in Escherichia coli. Science. 2010; 328:498–501. doi:10.1126/science.1185757. [PubMed: 20413500]
43. Helmstetter, CE., et al. Escherichia coli and Salmonella. Neidhardt, FC., editor. Vol. Vol. 2. ASM Press; 1996. p. 1627-1639.
44. Kuwada NJ, Cheveralls KC, Traxler B, Wiggins PA. Mapping the driving forces of chromosome structure and segregation in Escherichia coli. Nucleic Acids Res. 2013 doi:10.1093/nar/gkt468.

Europe PMC Funders Author Manuscripts

Europe PMC Funders Author Manuscripts

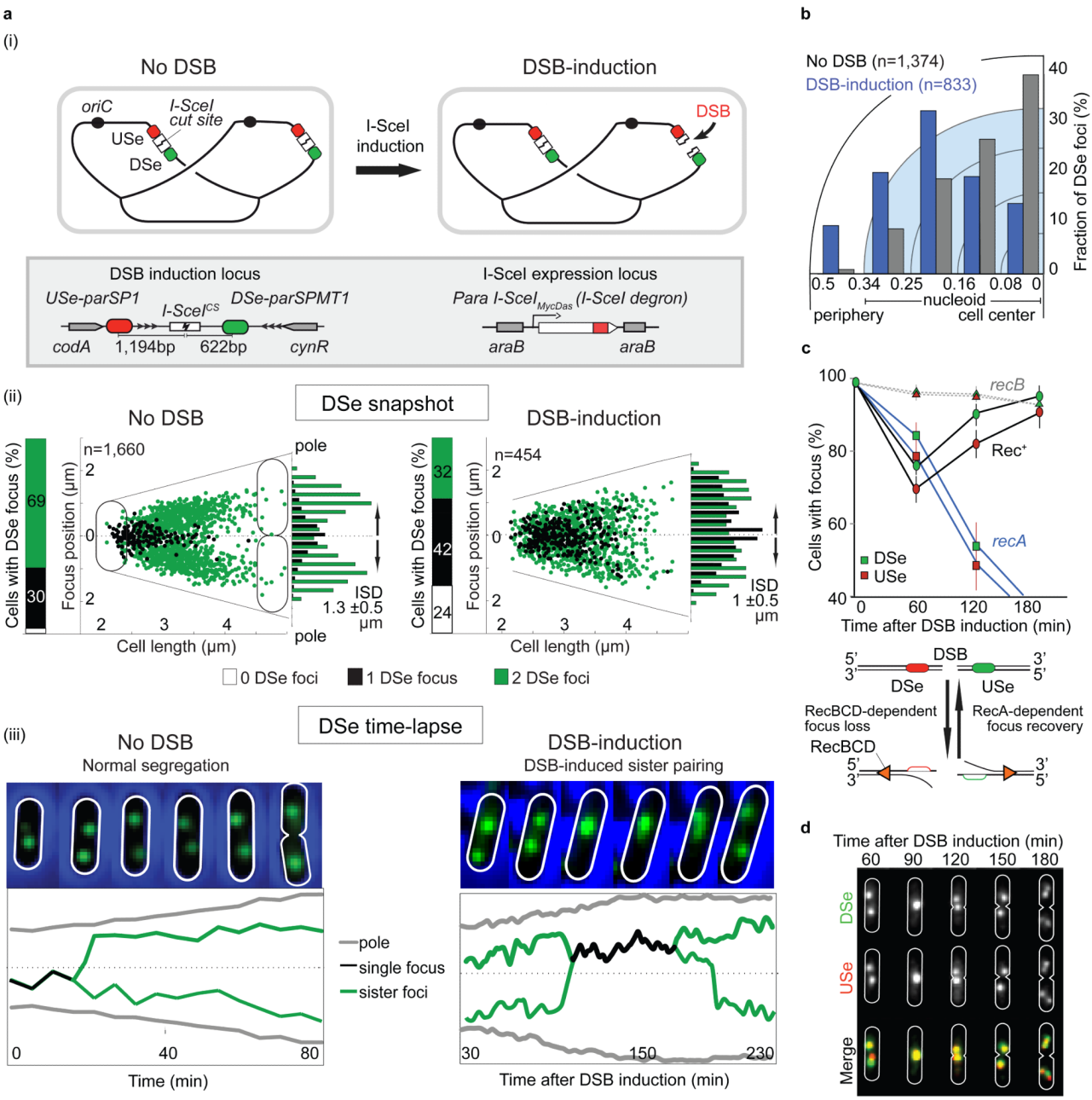

Figure 1. Effects of DSB-induction on positioning of adjacent chromosome loci

(a) (i) Schematic of DSB-induction. (ii) Snapshot analysis of DSe (Downstream end) localisation before (left) and after 60 min of DSB induction (right). ISD, mean Inter-Sister Distance. (iii), time-lapse analysis (5 min/frame) of DSe focus dynamics.

(b). Distributions of DSe foci along the cell diameter before and after 60 min of DSB induction. Data are shown for cut sites that changed position after DSB induction.

(c). DSB-induced reduction of the fraction of cells with DSe and USe foci is RecBCD-dependent and indicates simultaneous processing of both DSB ends.

(d). DSe and USe foci remain coincident during sister pairing and subsequent sister separation. In panels c and d, error bars indicate standard deviations.

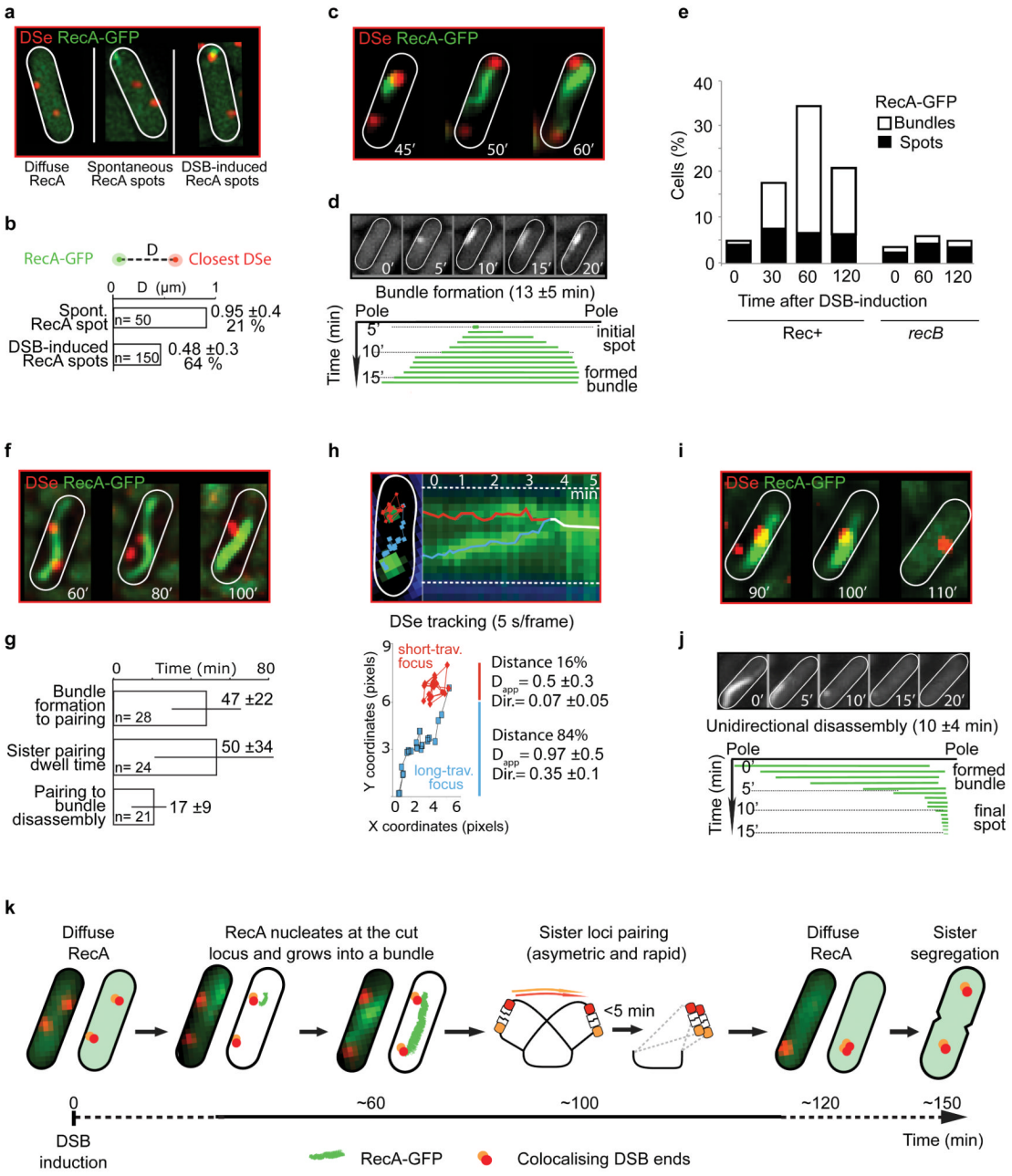

Figure 2. RecA bundle formation and disassembly, and RecA-mediated sister locus pairing

(a). RecA-GFP spot formation in relation to the cut locus during sister pairing using wide-field microscopy.

(b) Histograms of the mean distance (D) between the centres of RecA spots and the closest DSe focus with the percentage of colocalization (when D <0.5μm).

(c). Wide-field imaging of nucleation of RecA bundles from RecA-GFP spots at DSe.

(d) Time-lapse images and analysis of RecA-GFP bundle formation.

(e). Snapshot analysis of RecB-dependent RecA-GFP bundle formation as a function of DSB-induction time (500 cells analysed for each dataset).

(f). Wide-field imaging of RecA-GFP bundle prior to sister pairing.

Europe PMC Funders Author Manuscripts

(g) Histograms of the timing of bundle formation and disassembly as respect to sister pairing (time-lapse analysis; n events).
(h). Mobility of sister loci during sister pairing. DSe focus positions over 300 s time-lapse (5 s/frame) during pairing, with corresponding kymograph and mobility parameters. See Extended Data Figure 4 and Methods Online for definition and determination of directionality.
(i). Wide-field imaging of RecA-GFP bundle disassembly after DSe sister pairing.
(j) Time-lapse images and analysis of RecA-GFP bundle disassembly.
(k). Schematic of DSB-end and RecA dynamics during DSB repair by *E. coli* HR, based on integration of all data. In all panels, error bars indicate standard deviations.

Europe PMC Funders Author Manuscripts

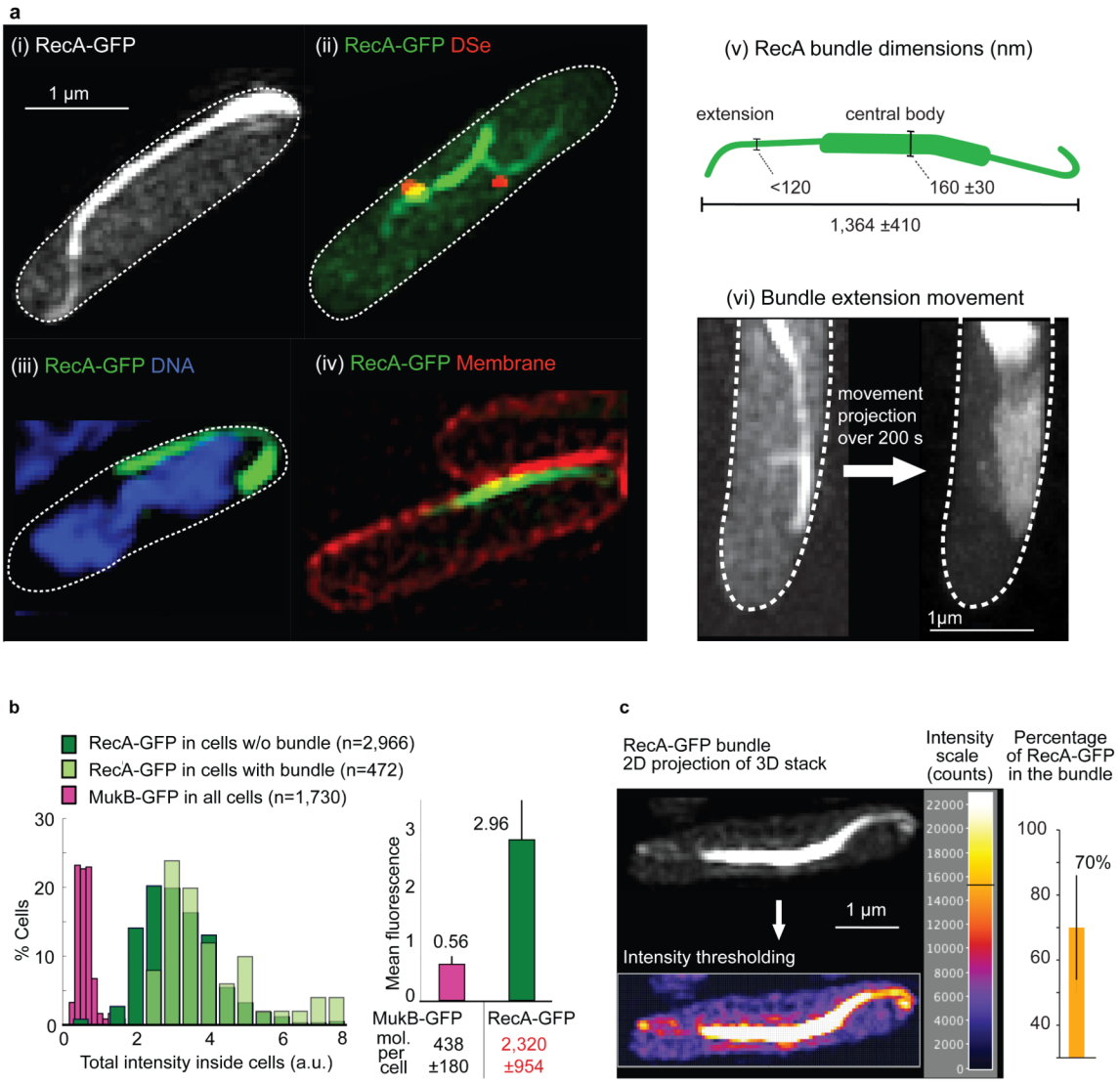

Figure 3. Super-resolution imaging of RecA bundles reveals their intracellular localization

(a). 3D-structured-illumination-microscopy (3D-SIM) of cells with DSB-induced RecA-GFP bundles alone (i), with DSe foci (ii), relative to DNA (iii), and to membrane (iv). (v), bundle architecture. (vi), the dynamic behavior of RecA bundle thin extensions is illustrated by the projection of the movement over 200s (taken from Video S7).

(b). Total fluorescence intensity distribution and average fluorescence of RecA-GFP in cells with or without bundles, and of MukB-GFP.

(c). The fraction of total cellular RecA monomers within bundles. See Online Methods. 70 ±18 % of the intracellular fluorescence was incorporated into bundles. Error bars indicate standard deviations in panels b and c.

Europe PMC Funders Author Manuscripts